

**Elektrotechnisches Institut (ETI)**Prof. Dr.-Ing. Michael Braun  
Prof. Dr.-Ing. Martin Doppelbauer  
Prof. Dr.-Ing. Marc Hiller  
Kaiserstr.12. 76131 Karlsruhe

Title:	Thermal Modeling of the Stator Slot in Electrical Machines Using an Extended Layer Approach
Authors:	Felix Hoffmann, Benedict Jux, Martin Doppelbauer
Institute:	Karlsruhe Institute of Technology (KIT) Institute of Electrical Engineering (ETI)
Type:	Conference Proceedings
Published at:	Proceedings IECON 2019 - 45th Annual Conference of the IEEE Industrial Electronics Society Publisher: IEEE Year: 2019 ISBN: 978-1-7281-4878-6 Pages: 1405–1410
Hyperlinks:	<a href="https://ieeexplore.ieee.org/document/8927002">https://ieeexplore.ieee.org/document/8927002</a>

© 2019 IEEE. Personal use of this material is permitted. Permission from IEEE must be obtained for all other uses, in any current or future media, including reprinting/republishing this material for advertising or promotional purposes, creating new collective works, for resale or redistribution to servers or lists, or reuse of any copyrighted component of this work in other works.

# Thermal Modeling of the Stator Slot in Electrical Machines Using an Extended Layer Approach

Felix Hoffmann, Benedict Jux, Martin Doppelbauer  
*Institute of Electrical Engineering (ETI)*  
*Karlsruhe Institute of Technology (KIT)*  
Kaiserstr. 12, 76131 Karlsruhe, Germany  
felix.hoffmann@kit.edu

**Abstract**—In the design process of efficient and high-power density machines, it is essential to couple the electromagnetic and thermal analysis. The thermal analysis can be done by numerical approaches or analytical lumped circuit analysis. The lumped circuit analysis has the advantage of a fast computation time, whereas the numerical approach has a high accuracy. In this paper an analytical approach for the stator slot is presented, which homogenizes the stator slot considering four directions in predefined layers. With the extension to model the layers in different directions, it is possible to predict a more precise temperature distribution inside the slot. Consequently, unlike the existing approaches, maximum and minimum temperatures can be predicted. We have implemented the extended layer approach, simulated and validated it with a Finite Element Analysis (FEA). The extended layer approach is simulated with six layers, which shows a good trade-off between accuracy and simulation time. The maximum temperatures of the hottest to the coolest layer differ by 21.8 K. The temperature difference between the different directions is up to 16.1 K, showing the importance of modeling the slot in all directions. The largest difference between the maximum temperatures of the FEA and the extended layer approach is 6.1 K in the transient case and 3.4 K in thermal steady state, whereas the average temperatures differ by a maximum of 3.5 K in the transient case and 0.2 K in thermal steady state. The validation with FEA results shows a good accordance to the analytical approach, while the simulation time of the analytical extended layer approach is about 150 times faster.

**Index Terms**—thermal modeling, lumped circuit, stator slot, layer approach

## I. INTRODUCTION

The trend in design of electrical machines is facing towards less volume and more efficient motors. Coming along with this, thermal modeling becomes more essential during the design process. The knowledge of the thermal behavior of an electrical machine is indispensable to determine the continuous and maximum power limit, as well as the continuous and maximum torque limit. In order to speed up the time to market, there exists a tendency to couple the electromagnetic and thermal design [1]. Two basic methods are used for thermal analysis: numerical approaches and analytical lumped circuit analysis [2]. The numerical method has the advantages of a high precision and the possibility of modeling any device geometry. However, the drawback is a high computation time and the need to set up a detailed Computer-Aided Design (CAD) model, where every single conductor including its

insulating lacquer needs to be considered [3]. In the contrary, the analytical approach has a very fast computation time. A main drawback is the need of setting up the lumped circuit in the design process, in which the main heat transfer paths have to be defined very accurately. This paper focuses on the analytical approach and the setup of a lumped circuit for the stator slot. Due to the commonly round wires inside the slot, it is very complex to model [4]. The heat path cannot be defined precisely and the exact location of the wires is unknown. However, the wires location has a minor influence on the temperature distribution for impregnated slots [5]. In order to deal with this uncertainty and the difficulty of the heat transfer between round wires, a layer approach is used to model the thermal behavior of the stator slot of an electrical machine. Certain areas are simplified to homogenized regions to predict the locationspecific temperature. There are already similar approaches available in literature [6], [7], where the slot is divided into a certain number of layers. The drawback of these approaches is that the layers are folded up, leading to an unidirectional heat flow model. As a result, the temperature is averaged over equidistant points from the slot center. Another method is to use an equivalent thermal conductivity to model the heat mechanisms in the stator slot [8], [9].

In this paper, we present an extended layer approach, which considers four directions inside the slot. In [6] the layers are folded up resulting in an unidirectional heat flow, leading to an averaging of the temperatures with equal distance to the slot's center. The extended approach gives a temperature distribution depending on the position inside the slot, leading to the possibility to determine maximum and minimum temperatures in addition to the average temperatures. Therefore, the extended approach provides a better prediction of hot spots in the slot, while maintaining a fast computation time.

## II. THERMAL MODELING

The presented extended layer model uses the method of homogenizing regions of the stator slot. As the real slot geometry contains commonly roundings, which are difficult to model, the geometry is simplified to a trapezoidal shape, maintaining the cross sectional area of the materials. The slot is divided in four directions: up, down, left and right. The division of the directions improves the accuracy of the temperature distribution inside the slot. Every direction consists

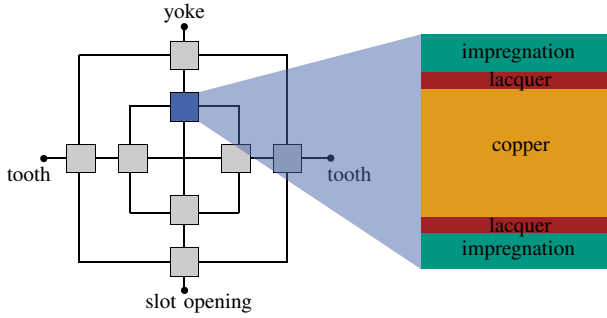


Fig. 1: Exemplary model structure in case of two layers.

of a predefined number of layers with equal width. Each layer itself includes one layer of copper and two layers of insulating lacquer and impregnation. For that reason, the layer model has impregnation in the center and at the outside of the stator slot. Fig. 1 presents an exemplary model structure in case of two layers. The thicknesses of the layers are computed such that the total cross sectional area of copper, impregnation, lacquer and insulating paper is consistent with the real geometry. Each layer has an equal percentage of the corresponding material. Every material layer is modeled with a thermal mass and thermal resistances in all four directions. To model the heat transfer only thermal conduction is regarded, which leads to the thermal resistance

$$R_{th} = \frac{d}{\lambda \cdot A}, \quad (1)$$

wherein  $d$  denotes the thickness,  $\lambda$  the thermal conductivity and  $A$  the cross sectional area of the material, where the heat flows through. The stator iron, consisting of two teeth and the yoke, is divided into different regions and homogenized over these. Every region is modeled with a thermal mass. We use a T-equivalent circuit [10] to model a distributed heat source in the stator iron and the copper layers. A negative resistance is connected between the thermal mass and the heat source to get a more precise average temperature of the copper and stator iron. Fig. 2 shows an example of a T-equivalent circuit in one dimension. The negative resistance is calculated by

$$R_{neg} = -\frac{1}{6} \frac{d}{\lambda \cdot A} = -\frac{R}{6}, \quad (2)$$

wherein  $R$  represents the total thermal resistance of the region in one direction given by (1). The stator consists of nine equal stator sectors. Due to its symmetry, the sectors behave thermally identical, leading to the same temperature at the interface between each other. If there is no temperature difference, the heat flow is equal to zero. Therefore, it is sufficient

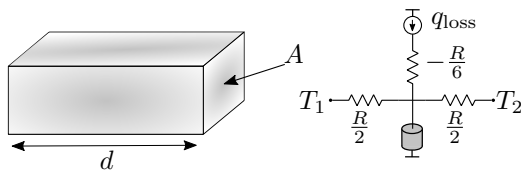


Fig. 2: Exemplary model of a T-equivalent circuit in one dimension.

to model only one stator section. As a result, the boundary condition of the stator section in tangential direction can be set to a perfectly insulating area. The surface area of the yoke is set to a constant temperature to model the stator cooling. Assuming a constant cooling temperature, there is no heat flow in axial direction since there is no temperature difference. Thus, the areas in axial direction are also modeled as perfect insulating areas. In radial direction, the air gap is assumed to be a perfect insulator due to the insulating characteristics of air. The iron loss density is assumed to be constant over the stator iron and the copper loss density is assumed to be constant over the windings. The copper losses are injected to the different layers with respect to their masses. Accordingly, any effect of the AC copper losses being larger in the region of the air gap is neglected [11]. We also assume that the thermal material characteristics are not dependent on temperature. The lumped circuit, including its boundary conditions, is set up in MATLAB<sup>®</sup> Simscape<sup>™</sup>. Hence, it is possible to analyze the transient behavior and analytically compute the temperature progression of the stator section over time.

### III. MACHINE UNDER TEST

The used machine is a Permanent Magnet Synchronous Motor (PMSM) with buried magnets and a tooth coil winding. The machine has a rotor and a stator cooling. It has three phases, three pole pairs and nine slots. Each slot includes 54 conductors with a diameter of 1.5 mm and an insulating lacquer with a thickness of 0.05 mm, leading to a copper filling factor of 56%. The modeled insulating paper is Trivoltorn NKN5202 and has a thickness of 0.2 mm. To increase the thermal conductivity among the windings, the slot is impregnated with Copaltec BR22. The copper length inside a slot is assumed to be 65.4% of the entire copper length. The rated electrical power of the machine is 17 kW.

We only consider a stator section of one slot pitch to analyze the thermal behavior inside a slot. Fig. 3 shows the cross sectional area of the analyzed stator section. Fig. 4 exposes the simplified trapezoidal geometry of the stator slot and an exemplary representation of the used extended layer approach for three layers. The machine parameters and the simplified geometry parameters are summarized in Table I. The material characteristics are essential to model the thermal behavior. The used values are based on literature. Table II summarizes the modeled material characteristics for the simulated stator section.

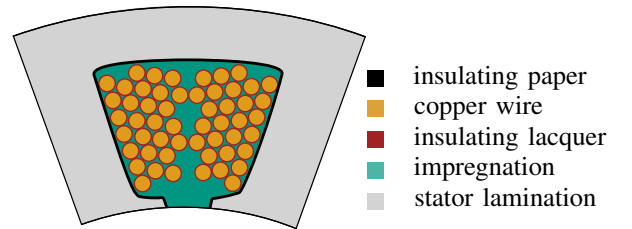


Fig. 3: Cross section of one slot pitch of the used machine.

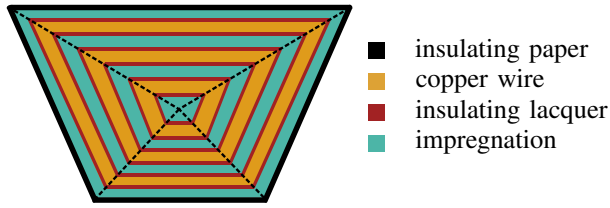


Fig. 4: Simplified geometry of the stator slot and exemplary representation of the extended layer approach for three layers.

TABLE I: Machine Parameters

Parameters	Values
number of pole pairs	9
rated power	17 kW
slot height	10.82 mm
upper slot width	17.48 mm
lower slot width	9.71 mm
inner stator diameter	56 mm
outer stator diameter	94.25 mm
filling factor	56 %
copper inside slot	65.4 %

TABLE II: Material Characteristics

Parameters	Values
thermal conductivity impregnation	0.9 $\frac{W}{mK}$
thermal conductivity copper	385 $\frac{W}{mK}$
thermal conductivity lacquer	0.22 $\frac{W}{mK}$
thermal conductivity insulating paper	0.2 $\frac{W}{mK}$
thermal conductivity stator iron	28 $\frac{W}{mK}$
specific heat capacity impregnation	300 $\frac{J}{kgK}$
specific heat capacity copper	368 $\frac{J}{kgK}$
specific heat capacity lacquer	368 $\frac{J}{kgK}$
specific heat capacity insulating paper	330 $\frac{J}{kgK}$
specific heat capacity stator iron	449 $\frac{J}{kgK}$
volumetric mass density impregnation	1050 $\frac{kg}{m^3}$
volumetric mass density copper	8900 $\frac{kg}{m^3}$
volumetric mass density lacquer	1100 $\frac{kg}{m^3}$
volumetric mass density insulating paper	1100 $\frac{kg}{m^3}$
volumetric mass density stator iron	7650 $\frac{kg}{m^3}$

#### IV. SIMULATION

In the following section the thermal model of the machine described in section III is set up, using the extended layer approach explained in section II, to simulate the thermal behavior within the slots. The temperature at the yoke's outer surface is set to 65 °C. The injected power is always based on the whole stator and consequently only a ninth is injected in the simulated model. The copper losses are the ohmic losses generated by the copper inside the slot. Fig. 5 shows the transient behavior of the copper temperature inside the side layers. The copper losses of  $P_{Cu} = 300$  W and the iron losses of  $P_{Fe} = 88$  W are applied at  $t = 30$  s. The simulated model includes six layers, where layer one marks the innermost layer and layer six the outermost layer. After the load step

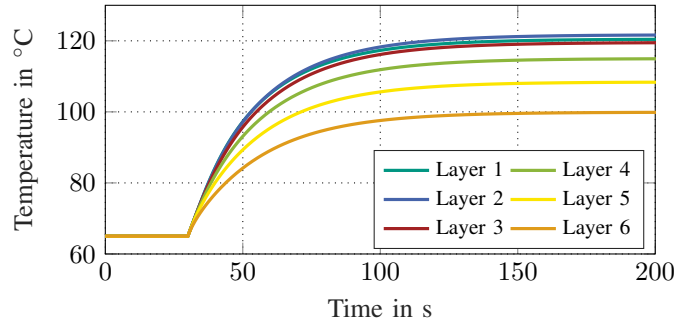


Fig. 5: Copper temperatures of the side layers for six layers and a load step of  $P_{Cu} = 300$  W and  $P_{Fe} = 88$  W at  $t = 30$  s.

at  $t = 30$  s, the temperatures of all layers rise with an initial slope of  $2.5 \text{ K s}^{-1}$ . This is due to the fact that the thermal mass  $C_{th}$  of one layer is proportional to the cross sectional area  $A$  in radial direction, whereas the thermal resistance  $R_{th}$  is inverse proportional to  $A$ . Therefore, the product of both is unchanged and the temperature slope after the load step is equal for the different layers. Thermal steady state is reached for all temperatures at about  $t = 180$  s. Because of the shortest thermal path to the cooling medium, the steady state temperature of layer six shows the coolest temperature of 99.9 °C. Layer two has the hottest temperature with 121.7 °C due to its longest thermal path. This leads to a total difference of the layer temperatures between the hottest and coolest layer of 21.8 K, which is about 38.45 % related to the temperature increase of  $\Delta T = 56.7$  K after the load step is applied. The temperature difference between each layer increases, if the layer is placed further out. This effect is due to the fact that the heat generated in the inner layers must flow through all outer layers. The temperature drop is proportional to the heat flow [12]. Thus, as the layer is placed further out, the temperature drop is higher.

##### A. Number of Layers

To examine the dependency of the number of layers, the steady state maximum, average and minimum temperatures inside the slot are observed for a load step of  $P_{Cu} = 300$  W and  $P_{Fe} = 88$  W. Fig. 6 presents the results for a varying

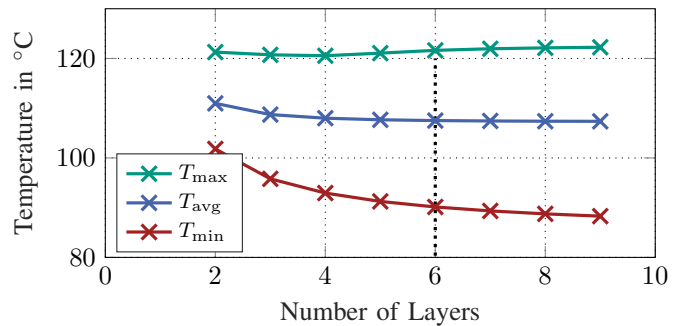


Fig. 6: Maximum, average and minimum copper temperatures of the slot for a variation of the layers from two to nine and a load step of  $P_{Cu} = 300$  W and  $P_{Fe} = 88$  W.

number of layers from two up to nine. With an increasing number of layers the temperatures saturate, leading to a maximum temperature  $T_{\max} = 122.3^\circ\text{C}$ , an average temperature  $T_{\text{avg}} = 107.4^\circ\text{C}$  and a minimum temperature  $T_{\min} = 88.3^\circ\text{C}$  for nine layers. To get a good trade-off between simulation time and accuracy of the model, we choose six layers for our model. The difference in temperature of the whole slot is 0.6 K for  $T_{\max}$ , 0.1 K for  $T_{\text{avg}}$  and 1.8 K for  $T_{\min}$ , whereas the simulation time is reduced by 26% in comparison to nine layers. For the following simulations, we keep using six layers for our slot model.

### B. Comparison of Temperatures in Different Directions

The main advantage of the presented model is the division in different directions, which provides a better prediction of the temperature distribution inside the slot. Fig. 7 shows the temperatures depending on the direction in layer six for a load step of  $P_{\text{Cu}} = 300\text{ W}$  and  $P_{\text{Fe}} = 88\text{ W}$  at  $t = 30\text{ s}$ . It also displays the layer approach used in [6], which homogenizes the temperatures of the directions in every layer, as a reference. The transient behavior directly after the load step is identical due to the compensating effect of the thermal mass and thermal resistance, leading to a constant temperature rise. The upper temperature reaches  $90.2^\circ\text{C}$  in steady state, whereas the side temperature and the down temperature reaches  $99.9^\circ\text{C}$  and  $106.3^\circ\text{C}$ , respectively. The upper temperature is the lowest, as the thermal path to the cooling medium is the shortest. The thermal path of the down layer has the highest thermal resistance, thus being the hottest region in the observed slot. The difference from the hottest point in layer six to the coolest point is given by 16.1 K, which is 39% compared to the total temperature step of the hottest point given by 41.3 K. The reference layer approach reaches in steady state  $97.9^\circ\text{C}$ , which is 8.4 K lower than the maximum temperature in the layer predicted by the extended layer approach. The minimum temperature of the sixth layer differs by 7.7 K. For this reason, the reference model can predict the average temperature of the layer, but is not meaningful for the maximum and minimum temperatures.

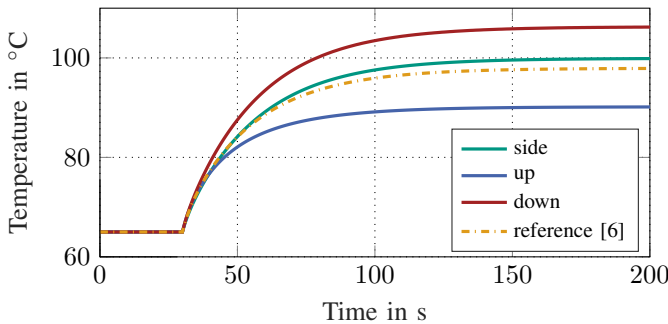


Fig. 7: Temperatures of the copper layers in all directions and a reference layer approach [6] for the outermost layer and a load step of  $P_{\text{Cu}} = 300\text{ W}$  and  $P_{\text{Fe}} = 88\text{ W}$  at  $t = 30\text{ s}$ .

### C. Copper Losses

Another factor, which affects the thermal behavior, is the amount of losses generated in the windings with a constant slot filling factor. Fig. 8 exposes the steady state values for the maximum, average and minimum temperatures for copper losses of  $P_{\text{Cu}} = 150\text{ W}$  up to  $P_{\text{Cu}} = 500\text{ W}$  and iron losses of  $P_{\text{Fe}} = 88\text{ W}$ . The maximum temperature  $T_{\max}$  inside the slot increases linearly from  $93.6^\circ\text{C}$  for a generated heat in the windings of  $150\text{ W}$  up to  $155.9^\circ\text{C}$  for copper losses of  $500\text{ W}$ . The average and minimum temperatures rise linearly from  $87.1^\circ\text{C}$  up to  $134.1^\circ\text{C}$  and from  $78.5^\circ\text{C}$  up to  $108^\circ\text{C}$ , respectively. This result matches with the basics of thermodynamics, which support that the temperature drop is proportional to the heat flow [12].

### D. Filling Factor

Depending on the slot copper filling factor, the slot's thermal behavior changes. Fig. 9 presents the effect of a varying filling factor inside a slot for a load step of  $P_{\text{Cu}} = 300\text{ W}$  and  $P_{\text{Fe}} = 88\text{ W}$ . The maximum temperature  $T_{\max}$  decreases linearly from  $138.3^\circ\text{C}$  for a filling factor of 25% down to  $117.2^\circ\text{C}$  for a filling factor of 65%, which is a reduction of 28.8% compared to the initial temperature rise. The average and minimum temperatures decrease linearly from  $116.2^\circ\text{C}$  to  $105.1^\circ\text{C}$  and from  $91.9^\circ\text{C}$  to  $89.8^\circ\text{C}$ , respectively. The decreasing behavior is due to an increased overall thermal conductivity. The resulting thermal conductivity of the slot is increased as the amount of impregnation with a low thermal conductivity is reduced and the amount of copper with a high thermal conductivity is increased.

## V. VALIDATION

To validate the results presented in the previous section, we have set up and analyzed a Finite Element Analysis (FEA) model of the stator section in Ansys Mechanical<sup>®</sup>. In the FEA the original geometry of the stator section is studied. The assumptions and boundary conditions in the FEA are the same as the ones used for the extended layer approach, explained in section II. Three load steps are applied to compare the results. The first one is applied at  $t = 30\text{ s}$  with a generated heat in the windings of  $P_{\text{Cu}} = 300\text{ W}$  and

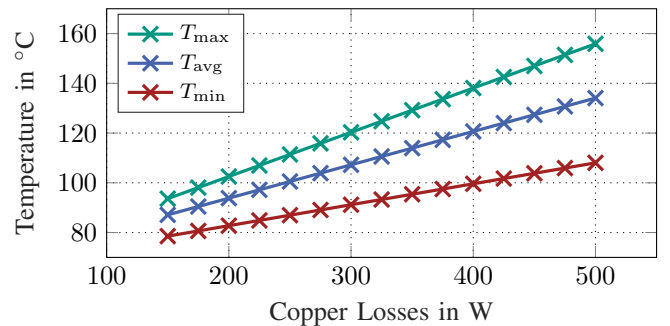


Fig. 8: Maximum, average and minimum copper temperatures of the slot for a copper loss variation of  $P_{\text{Cu}} = 150\text{ W}$  up to  $P_{\text{Cu}} = 500\text{ W}$  and a constant iron loss of  $P_{\text{Fe}} = 88\text{ W}$ .



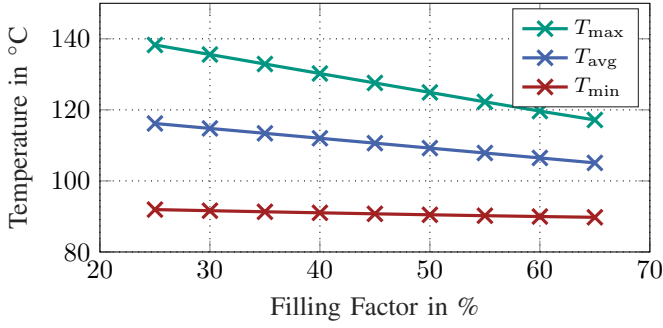


Fig. 9: Maximum, average and minimum copper temperatures of the slot for a copper filling factor variation of 25% up to 65% for a load step of  $P_{Cu} = 300$  W and  $P_{Fe} = 88$  W.

reduced to  $P_{Cu} = 250$  W at  $t = 110$  s. The third load step is applied at  $t = 200$  s with a generated heat in the windings of  $P_{Cu} = 350$  W. The iron losses of  $P_{Fe} = 88$  W are applied at  $t = 30$  s and stay constant afterwards. Fig. 10 exposes the resulting maximum, average and minimum temperatures over time for the FEA and the modeled extended layer approach. The maximum, as well as the average and minimum temperatures of the analytical model have a smaller time constant than the temperatures computed through the FEA, which can be seen throughout the steeper rise and a steeper declination of the temperatures. After the first load step the analytically computed temperatures rise with a constant of  $2.4$  K s<sup>-1</sup>, whereas the FEA results show a slope of  $2.2$  K s<sup>-1</sup>. The maximum temperatures differ by a maximum of 6.1 K in the transient case. The average and minimum temperatures differ by a maximum of 3.5 K and 2.5 K. At thermal steady state, reached at  $t = 300$  s, the maximum temperature of the analytical model is given by 130.4 °C, which is 3.4 K higher than the temperature resulting from the numerical approach. The average temperature reaches 114.1 °C, which is 0.2 K lower than the numerical result. The minimum temperature of the analytical solution reaches

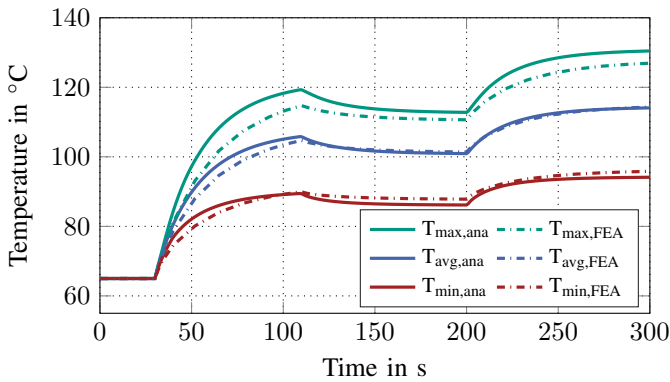


Fig. 10: Maximum, average and minimum copper temperatures of the stator slot of the analytical approach with six layers (solid) and the numerical results (dashed) for load profile of  $P_{Cu} = [300\ 250\ 350]$  W and  $P_{Fe} = 88$  W starting at  $t = 30$  s.

94.1 °C, which is 1.7 K lower than the temperature computed in the FEA. It is uncritical to overestimate the maximum temperature inside the slot. This gives a margin for possible residual air quantities after impregnation inside the slot, which increases the maximum temperature. The extended layer approach assumes the impregnation to be equally distributed inside the slot, whereas the real geometry has a relatively high amount of impregnation in the center of the slot (see Fig. 3). For that reason, there is a difference in the maximum temperature between the analytical and numerical approach. As the impregnation has a low thermal conductivity, the heat generated in the copper windings has a lower thermal resistance towards the cooling system. If more impregnation is in the center of the slot, the maximum temperature decreases. The reason for a lower minimum temperature in the extended layer approach is similar to the above explained behavior. For the real geometry, a high amount of impregnation is placed at the top of the slot. This results in a higher thermal resistance towards the cooling system for the outer windings and therefore, also to a higher minimum temperature. For the boundary temperatures of the slot a comparison of the temperatures in the stator iron is also needed. Fig. 11 shows a comparison of the maximum, average and minimum stator iron temperature of the FEA and the extended layer approach. The applied load is the same as described before. The minimum stator iron temperature stays at 65 °C for the analytical approach and the FEA, as the applied boundary condition at the outer stator diameter is 65 °C. The average temperature reaches a steady state value of 73.6 °C at  $t = 300$  s, which is 0.6 K lower than the value computed with the FEA. The maximum temperature computed analytically rises faster than the one of the FEA and reaches a steady state value of 88 °C at  $t = 300$  s, which is 2 K lower than the value computed with the FEA. The stator is homogenized into defined regions in the analytical approach. In the contrary, the FEA uses a finer mesh, which allows a better detection of hot spots and explains the temperature difference. It is not relevant to determine the hot

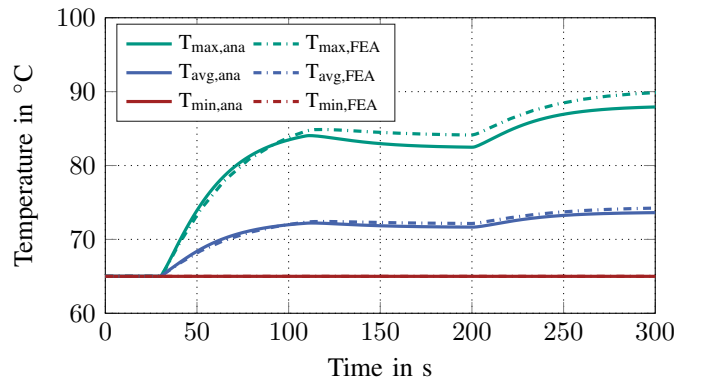


Fig. 11: Maximum, average and minimum stator iron temperatures of the analytical approach with six layers (solid) and the numerical results (dashed) for load profile of  $P_{Cu} = [300\ 250\ 350]$  W and  $P_{Fe} = 88$  W starting at  $t = 30$  s.

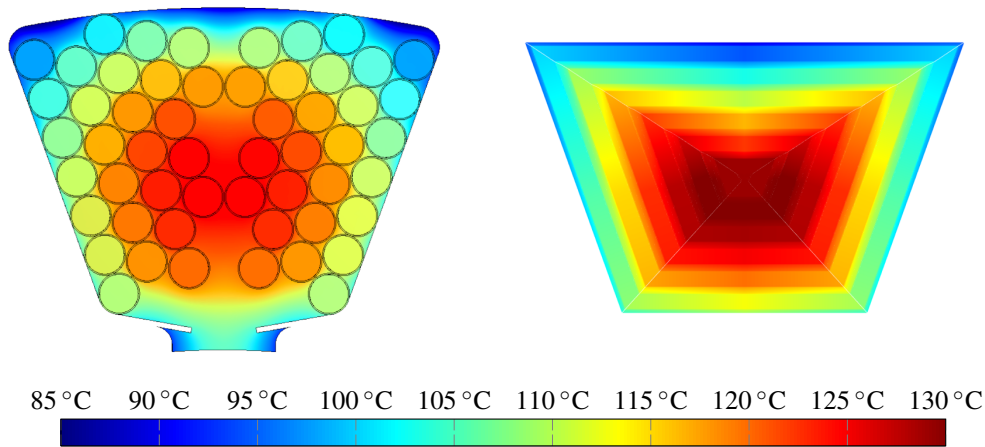


Fig. 12: Temperature distribution comparison of the numerical approach on the left side and the analytical approach on the right at  $t = 300$  s for a load profile of  $P_{Cu} = [300\ 250\ 350]$  W and  $P_{Fe} = 88$  W.

spots in the stator very accurately. The average temperature, which can be estimated precisely, is of high interest to set the boundary conditions for the stator slot accurately. To observe the temperature distribution inside the slot, Fig. 12 presents a comparison of the FEA and the analytical approach at  $t = 300$  s for the load profile described before. It is visible that the hottest spot of the slot is not directly in the slot's center, but further down. This is because the second down layer has a longer thermal path to the cooling medium than the first one. The temperature distribution of the analytical model shows good accordance to the distribution calculated by the FEA.

The analytical model implemented in MATLAB® Simscape™ is about 150 times faster than the FEA calculation and takes about 9.5 s for the presented load profile.

## VI. CONCLUSION AND FUTURE WORK

We have extended an existing layer approach to get the information of the temperature distribution in all directions. This leads to a better prediction of the local temperatures and the possibility to detect the maximum and minimum temperatures inside the stator slot. We have determined that the choice of six layers gives a good trade off between accuracy and simulation time. For a load step of  $P_{Cu} = 300$  W and  $P_{Fe} = 88$  W the maximum temperature inside the slot is  $121.7^\circ\text{C}$ , which is  $21.8$  K hotter than the hottest outermost copper layer. The directions have a temperature difference between the upper layer to the side layer of  $16.1^\circ\text{C}$ , which is about 39% compared to the total temperature rise. The reference layer approach can therefore only predict the average slot temperature, whereas with the extended layer approach a prediction of the maximum and minimum temperatures is possible. For an increasing filling factor, the temperatures decrease linearly, whereas the temperatures increase linearly for higher copper losses. The validation with the FEA results shows a good accordance to the analytical approach, whereas the simulation time of the analytical approach is about 150 times faster. The maximum temperature of the slot differs by

a maximum of  $6.1$  K in the transient case and by  $3.4$  K in steady state. The average and minimum temperatures differ by a maximum of  $3.5$  K and  $2.5$  K in the transient case and by  $0.2$  K and  $1.7$  K in steady state.

Currently we are setting up a test bench to validate the simulation results with measurements. In our future work, we will be implementing the extended layer approach to model the end windings.

## REFERENCES

- [1] A. Boglietti, A. Cavagnino, and D. Staton, "Determination of critical parameters in electrical machine thermal models," *IEEE Transactions on Industry Applications*, vol. 44, no. 4, pp. 1150–1159, 2008.
- [2] P. H. Mellor, D. Roberts, and D. R. Turner, "Lumped parameter thermal model for electrical machines of tefc design," *IEE Proceedings B - Electric Power Applications*, vol. 1991, 1991.
- [3] S. Oechslen, *Thermische Modellierung elektrischer Hochleistungsantriebe*. Wiesbaden: Springer, 2018.
- [4] A. Boglietti, A. Cavagnino, D. Staton, M. Shanel, M. Mueller, and C. Mejuto, "Evolution and modern approaches for thermal analysis of electrical machines," *IEEE Transactions on Industrial Electronics*, vol. 56, no. 3, pp. 871–882, 2009.
- [5] David James Powell, "Modelling of high power density electrical machines for aerospace," 2003.
- [6] D. A. Staton, "Thermal computer aided design-advancing the revolution in compact motors," in *Electric Machines and Drives Conference, 2001. IEMDC 2001. IEEE International*. IEEE / Institute of Electrical and Electronics Engineers Incorporated, 2001, pp. 858–863.
- [7] D. Staton, A. Boglietti, and A. Cavagnino, "Solving the more difficult aspects of electric motor thermal analysis in small and medium size industrial induction motors," *IEEE Transactions on Energy Conversion*, vol. 20, no. 3, pp. 620–628, 2005.
- [8] Z. Hashin and S. Shtrikman, "A variational approach to the theory of the effective magnetic permeability of multiphase materials," *Journal of Applied Physics*, vol. 33, no. 10, pp. 3125–3131, 1962.
- [9] G. W. Milton, "Bounds on the transport and optical properties of a two-component composite material," *Journal of Applied Physics*, vol. 52, no. 8, pp. 5294–5304, 1981.
- [10] T. A. Lipo, *Introduction to AC machine design*, ser. IEEE Press series on power engineering. Hoboken, New Jersey: Wiley IEEE Press, 2017, vol. 63.
- [11] P. B. Reddy, T. M. Jahns, and T. P. Bohn, "Transposition effects on bundle proximity losses in high-speed pm machines," in *IEEE Energy Conversion Congress and Exposition, 2009*. Piscataway, NJ: IEEE, 2009, pp. 1919–1926.
- [12] A. F. Mills, *Heat transfer*, 2nd ed. Upper Saddle River, NJ: Prentice Hall, 1999.